E9-2021-51

I. N. Kiyan, A. F. Chesnov, V. L. Smirnov,
D. S. Petrov, R. V. Galkin, S. B. Fedorenko,
A. S. Vorojtsov, J. Sulikowski [1], P. Bogdali [1]

DIPOLE MAGNET **M1** OF THE BEAM TRANSPORTATION LINE OF THE **AIC-144** CYCLOTRON

[1] Institute of Nuclear Physics of the Polish Academy of Sciences, Krakow, Poland

Киян И. Н. и др. E9-2021-51

Дипольный магнит M1 линии транспортировки пучков циклотрона АИЦ-144

В работе приведены результаты анализа линий транспортировки пучка многоцелевого изохронного циклотрона АИЦ-144, расположенного в ИЯФ ПАН (Краков, Польша). Представлен новый поворотный магнит M1, изготовленный в Научно-производственном объединении «Атом» и ЛЯП ОИЯИ (Дубна) и предназначенный для работы в системе транспортировки пучков циклотрона АИЦ-144. Показана технология изготовления магнита M1, и приведены результаты проведенных магнитных измерений. С целью оценки влияния выявленного отклонения измеренного поперечного магнитного поля от расчетного на расчетной карте магнитного поля проведен расчет динамики пучков для основного режима работы циклотрона АИЦ-144: p, $E_k = 60{,}7$ МэВ. Результаты расчета показали, что новый поворотный магнит M1 позволяет повернуть пучок на заданный угол с регулировкой в диапазоне от 68 до 70° при рабочем токе в диапазоне от 250 до 270 А соответственно. В результате было установлено, что пучок протонов соответствует предъявляемым к нему требованиям.

Работа выполнена в Лаборатории ядерных проблем им. В. П. Джелепова ОИЯИ.

Сообщение Объединенного института ядерных исследований. Дубна, 2021

Kiyan I. N. et al. E9-2021-51

Dipole Magnet M1 of the Beam Transportation Line of the AIC-144 Cyclotron

The paper presents the analysis results of the beam transportation lines of the multipurpose isochronous cyclotron AIC-144 located at the INP PAS (Krakow, Poland). Also, the paper presents the new M1 bending magnet, manufactured at the Research and Production Association “Atom” and DLNP JINR factories (Dubna) and assigned to operate in the beam transportation system of the AIC-144 cyclotron. The paper shows both the manufacturing technology of the M1 magnet and the results of the magnetic measurements. In order to evaluate the influence of revealed deviation of the measured transverse magnetic field from the calculated one, the beam dynamics was calculated using the calculated magnetic field map for the main operating mode of the AIC-144 cyclotron: p, $E_k = 60.7$ MeV. The calculation results showed that the new M1 bending magnet allows the beam rotation at a given angle with adjustment in the range from 68° to 70° at a working current in the range from 250 to 270 A respectively. As a result, it was found that the proton beam meets the requirements for it.

The investigation has been performed at the Dzhelepov Laboratory of Nuclear Problems, JINR.

Communication of the Joint Institute for Nuclear Research. Dubna, 2021

INTRODUCTION

The system for transporting beams of the multipurpose isochronous cyclotron AIC-144 (INP PAS, Krakow, Poland) consists of the following magnetic elements: dipoles and quadrupoles. The bending magnet M1 is used to deflect the beam from the AIC-144 cyclotron to the adjacent experimental hall, where the system for dividing the transportation line into two beam tracts is located. The first is used to deliver the proton beam to the eye melanoma treatment room. The second is under development and is intended to deliver the beam to the site of executing various physical experiments. The bending magnet M2 is used to switch between the two beam tracts (Fig. 1). The medical beam's transportation line (from the M2 bending magnet) consists of two doublets of magnetic quadrupoles, beam diagnostics system (beam's visual diagnostics system and beam current sensors), and equipment for beam preparation (mixers, collimators, stoppers). The experimental beam's transportation line (from the M2 bending magnet) consists of one doublet of magnetic quadrupoles and beam diagnostics system (beam's visual diagnostics system and beam current sensor). The beam transportation line from the AIC-144 cyclotron to the bending magnet M2 consists of two doublets

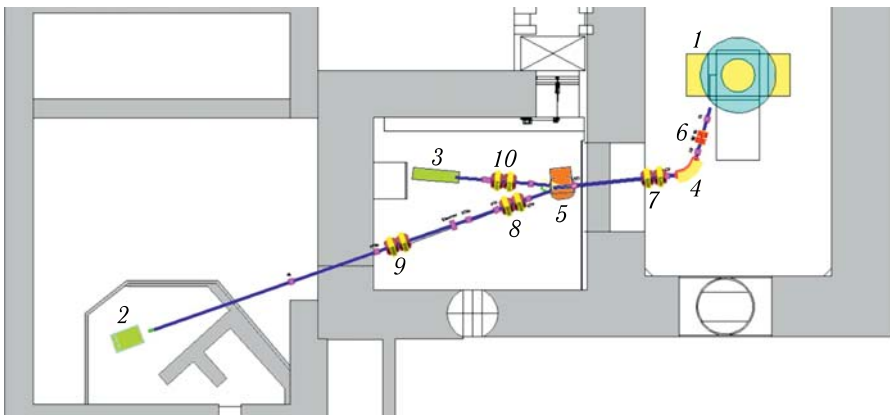

Fig. 1. Beam transportation system of the AIC-144 cyclotron: *1* — cyclotron, *2* — room for treatment of eye melanoma, *3* — stand for physical experiments, *4* — bending magnet M1, *5* — bending magnet M2, and *6–10* — quadrupole doublets

of magnetic quadrupoles, mixers, beam's visual diagnostics system, beam current sensors, and the bending magnet M1.

The development program of the AIC-144 accelerator facility includes the modernization and optimization of the beam transportation system, in particular, replacement of the M1 and M2 dipole magnets. The bending magnets M1 and M2 (dipoles), which are currently used, have a lot of significant drawbacks, the main of which are the lack of proper functionality, high power consumption, and non-optimal work from the point of view of beam optics.

The main problem with the existing bending magnet M1 is that the radius of curvature of the magnet's center line does not match the structure of the beam transportation line. To match the beam deflected by the dipole with the further tract, specially made flanges with beveled edges are used. This system does not provide optimal transportation of beam. Also, the dipole has a complex system for adjustment of the edge focusing beam. The adjustment is carried out using the spatial displacements of the parts of the magnet poles. The magnetic masses located at the edges of the poles rotate and shift with the help of the external rods. There is no visual assessment of the installed positions of these magnetic elements, as well as their diagnostics, which complicates the process of adjusting the position and form of the beam cross section on the M1 magnet exit. The analysis of the beam current measured by the sensors installed in the beam transportation line shows that the beam current intensity when passing from the AIC-144 cyclotron to the end point in the room for eye melanoma treatment is reduced by 20 %. All losses are concentrated after the M1 bending magnet. It is not possible to establish the exact location of these losses due to insufficient number of the installed beam current sensors. The analysis of the beam envelopes (Fig. 2) shows that there are two possible areas where the beam can perish due to the apertures sizes of the structural elements. The first area is located behind the M1 bending magnet at the location of the beam stopper. The second possible place of losses can be in the area of doublet of magnetic quadrupoles located behind the M2 bending magnet, where the transverse dimensions of the beam are greatest.

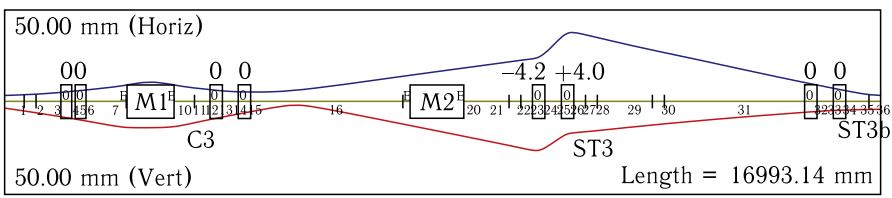

Fig. 2. Beam envelopes (in the beam transportation line from the AIC-144 cyclotron to the room for eye melanoma treatment) obtained using the Trace3D program [1]. The graph shows the main positions of visual inspection of the beam's cross-sectional shape. Also shown are the values of magnetic fields in quadrupole doublets in units of T/m

The beam misalignment with the transportation system, difficulties with the formation and positioning of the beam are associated with the described disadvantages of the existing M1 bending magnet. The new M1 bending magnet, manufactured by "Atom" (Dubna, Russia) and DLNP JINR (Dubna) factories, was designed at DLNP JINR in accordance with the terms of technical task approved by the management of the AIC-144 cyclotron department (INP PAS, Krakow, Poland). This magnet should improve the beam dynamics in the beam transportation system as well as increase the final intensity of beam current.

1. THE M1 MAGNET PARAMETERS

The new M1 bending magnet, according to the technical task, deflects a proton beam with an energy up to 60.7 MeV at an angle of 68–70° along the arc with a radius of curvature of 840 mm. The magnitude of magnetic field at the central point (along the centers of the poles in the median plane of the M1 bending magnet) when operating with the maximal energy of beam is 1.33 T. The magnet yoke is C-type (Fig. 3). Structurally, it consists of three parts: a vertical bar, a horizontal yoke (upper and lower), and a pole (upper and lower). The magnet height is 660 mm. The horizontal yoke and vertical bar have the azimuth dimension of 70°. The axial gap between the poles is 50 mm. The material of the yoke is st. 10. The weight of the assembled magnet is 2.4 t.

Analysis of the beam envelopes in the beam transportation line and analysis of the readings of the beam diagnostics system allow us to conclude that the existing M1 bending magnet has edge plates adjustment corresponding to the rotation of the pole edges by $+/-20\div25°$ relative to the radius vectors, which bound the yoke of the magnet. This provides additional edge focusing of the beam in the vertical direction. The transverse dimensions of the beam at the exit from the dipole meet all the basic requirements. Therefore, in the new design of the M1 bending magnet the similar edge focusing of the beam was conserved. For this purpose, the poles of the M1 bending magnet have the bevels with an angle of

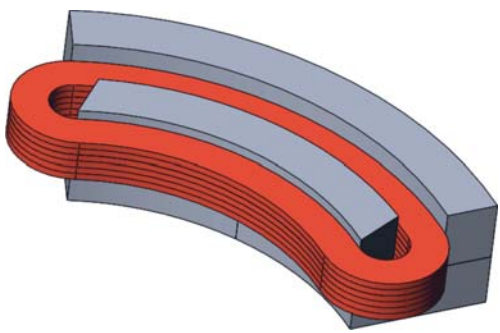

Fig. 3. Three-dimensional model of the M1 bending magnet

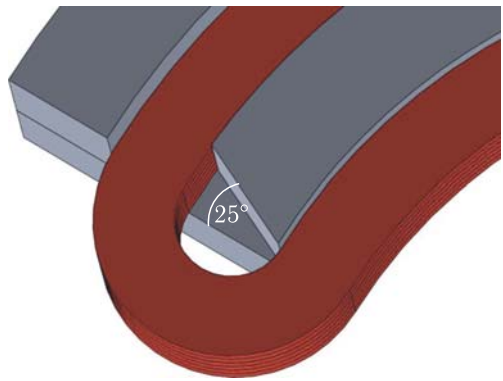

Fig. 4. Organization of additional edge focusing of the beam by the bevels of the poles

+/−25° relative to the radius vectors, which bound the yoke of the magnet (Fig. 4).

The magnetic field is generated by two water-cooled semi-windings. Each semi-winding consists of six double galettes (11 turns per layer), wound with the copper conductor 8.5 × 8.5 mm, Ø5.3 mm. The dimensions of the cross section of the dipole magnet M1 and the structure of semi-winding are shown in Fig. 5.

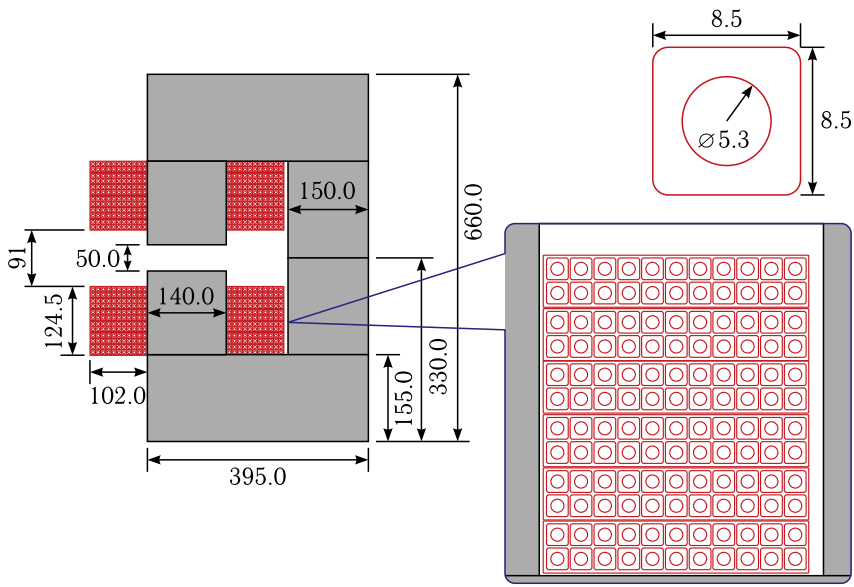

Fig. 5. Cross section of the dipole magnet M1

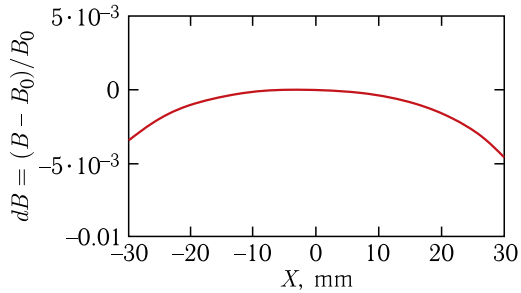

Fig. 6. Transverse inhomogeneity of the magnetic field of the M1 bending magnet

The transverse and vertical sizes of the beam during passing the dipole magnet M1 do not exceed ±15 mm. To ensure the dynamic requirements, it is sufficient to have transverse magnetic field in the working area ±20 mm with an inhomogeneity not exceeding $2.0 \cdot 10^{-3}$ in absolute value. The designed structure allows satisfying the given criterion (Fig. 6).

In this and other graphs with transverse inhomogeneities and magnetic fields "0" corresponds to the crossing of the OX axis with the projection of the longitudinal center line of the pole on the median plane of the M1 bending magnet (magnet's central point). The OX axis is directed from the curvature center of the M1 bending magnet. The calculation of the three-dimensional magnetic field was carried out using the Opera3D program [2].

Figure 7 shows the new M1 bending magnet manufactured by "Atom" (Dubna, Russia) and DLNP JINR (Dubna) factories.

Fig. 7. New M1 bending magnet

2. THE M1 MAGNET CHARACTERISTICS

By water, the galettes are fed in parallel from the water collector located on the M1 magnet yoke (similarly to the design of the old M1 magnet) (Fig. 7). Water supply/drainage is carried out through hoses Dy 13.5 mm. By electricity, the galettes are connected in series using the corresponding jumpers. A power supply (current source) is connected to the semi-windings similarly to the design of the old M1 magnet. The cleats with holes Ø 8.5 mm are used. Each of the galettes has the thermorelay with actuation / letting go temperature of 55/45°C. The thermorelay connection is in series and the assembly outputs are connected to a special connector.

Table 1. **M1 magnet characteristics**

Parameter	Value
Number of windings	2
Number of galettes in a winding	6
Number of turns in a galette	22
Total number of turns	$22 \cdot 6 \cdot 2 = 264$
Conductor type	Cu; 8.5×8.5 mm; Ø 5.3 mm
Conductor length in one galette	63 m
Nominal DC current (protons 60.7 MeV)	~ 250 A
Voltage on windings	70.44 V
Total power consumption	17.61 kW
Nominal current density	~ 5 A/mm^2
Total cooling water consumption from parallel collector (at pressure drop of 4 atm)	22.12 L/min
Cooling water outlet temperature (inlet temperature 25°C)	36.4°C
Yoke and poles material	steel 10
Windings weight	$166 \cdot 2 = 332$ kg
The weight of the assembled magnet	~ 2.4 t
Azimuth dimension	70°
Curvature radius	840 mm
Third-party software	Opera3D
Measured pole-to-pole gap	(50.03 ± 0.05) mm
Measured magnetic field in the magnet's central point	~ 1.33 T

3. THE M1 MAGNET MANUFACTURE

The M1 magnet yoke was manufactured by "Atom" (Dubna, Russia) factory. The winding of galettes and the M1 magnet's assembly were carried out at DLNP JINR (Dubna) factory. The galettes were wound using the CH-10C-1200 machine with automatic laying insulation on the conductor. The

Fig. 8. Winding machine CH-10C-1200

Fig. 9. DLNP furnace for baking galettes

conductor insulation is glass tape with the hot cured epoxy compound 0.2 mm thick per side. The glass textolite sheets with a thickness of 0.5 mm were laid between the galettes. The glass textolite sheets with a thickness of 0.5 mm were also laid between the galettes and the side surfaces of the poles, as well as between the galettes and the yoke's vertical bar. After the galettes were impregnated with epoxy compound, each of the galettes was baked in the DLNP furnace at a temperature of 160 °C. Figures 8 and 9 show the CH-10C-1200 winding machine and the DLNP furnace for baking galettes.

After assembling, the control measurements of geometrical sizes of the M1 magnet, especially pole-to-pole gap, were carried out. The measured value of the gap is $h = (50.03 \pm 0.05)$ mm. Thus, the manufacturing and assembly accuracy of the M1 magnet is fully consistent with the technical task for its manufacture. (According to the technical task the pole-to-pole gap value must be $h = (50 \pm 0.05)$ mm.)

The voltage drop measurements per each of the galettes were carried out for coil current $I = 309.4$ A. Table 2 shows the results of these measurements.

No. is the galette number. U is voltage drop per galette. Maximal difference is 0.1 V. The voltage drop per turn is ~ 0.3 V/turn. Therefore, we can conclude that there are no short circuits between the turns.

Table 2. **The voltage drop per galette**

No.	1	2	3	4	5	6	7	8	9	10	11	12
U, V	6.57	6.59	6.6	6.63	6.63	6.59	6.64	6.65	6.67	6.65	6.65	6.58

4. THE M1 MAGNET'S MAGNETIC MEASUREMENTS AND THEIR ANALYSIS

The magnetic measurements were carried out for the new M1 magnet using the available magnetic measurement system located in the Scientific and Experimental Department of New Accelerators, DLNP, JINR. This system allows magnetic measurements in a Cartesian coordinate system only. Therefore, full-scale measurements of the magnetic field map in the median plane of the M1 magnet were not carried out. The magnetization curve at the central point and the magnetic field along the transverse axis in the median plane of the M1 magnet were measured. Magnetic measurements were carried out on the upper half of the hysteresis loop in an automated mode using the Hall magnetometer: LakeShore 475 DSP Gaussmeter. The magnetometer was controlled from the computer via the RS-232C serial interface. Control program: MFMP 2021 (Magnetic Field Measurement Program 2021) was written in the C++ in the MS Visual Studio 2019 programming environment using parallel computing technology. The Hall sensor was previously calibrated at the Scientific and Technological Department of Accelerators, FLNR, JINR, using the nuclear magnetometer: MetroLab precision NMR Teslameter 2025. The calibration magnet, which sets the magnetic field in the range from 0 to 2.9 T, was used. The calibration magnet's power supply is EVPU PS 1200-40. The zero setting of the Hall magnetometer before calibrating the Hall sensor was performed using a 0-Gauss camera, and before each of the rest of magnetic measurements it was performed relative to the Earth's magnetic field. Figures 10 and 11 show the processes of the Hall sensor calibration and the M1 magnet's magnetic measurements.

The measured calibration straight line is shown in Fig. 12.

Fig. 10. Hall sensor calibration in the experiment dated 02.06.2021

Fig. 11. M1 magnet's magnetic measurements in the experiment dated 28.06.2021

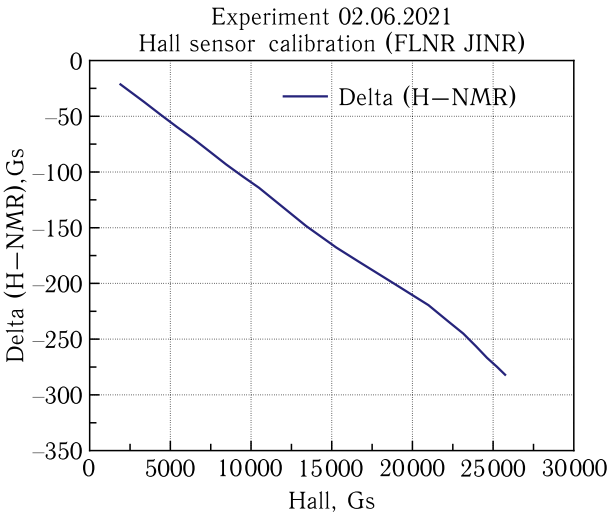

Fig. 12. Measured calibration straight line in the experiment dated 02.06.2021

The calibration straight line is the difference between the readings of the Hall magnetometer and the readings of the NMR magnetometer, taken depending on the readings of the Hall magnetometer. The measured magnetization curve of the M1 magnet is shown in Fig. 13.

Curves *1* and *2* respectively show values measured using the Hall magnetometer and recalculated using the measured calibration straight line.

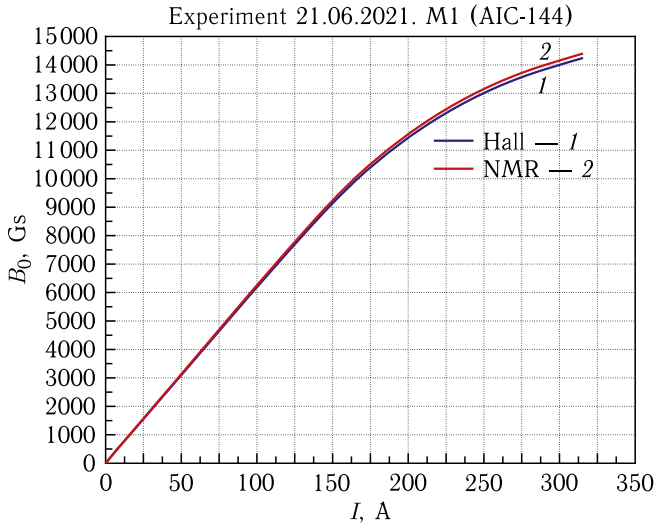

Fig. 13. The measured magnetization curve of the M1 magnet in the experiment dated 21.06.2021

The difference between the calculated and measured magnetic field values at the central point of the M1 magnet was less than 1% at the working current $I = 250$ A. After bringing the measured values to calculated ones, some noticeable difference between calculated and measured values of the transverse magnetic field was detected. The transverse magnetic field is evaluated along the transverse axis in the median plane of the M1 magnet. The difference is observed in the range from the central point to the vertical bar of the M1 magnet yoke. This vertical bar has noticeable influence on the M1 magnet's magnetic field that was not taken into account in the calculations. Figure 14 shows the calculated and measured transverse magnetic fields of the M1 magnet. Figure 15 shows calculated and measured inhomogeneities of the M1 magnet's transverse magnetic field.

Similar magnetic measurements were carried out in parallel of the transverse axis of the M1 magnet with the shift of the Hall sensor relative to the transverse axis of the M1 magnet upward by 10 and 15 mm, and also downward, respectively. The measurement results showed that the median plane of the magnetic field is shifted relative to the median plane of the M1 magnet downward by 1 mm, which corresponds to the positioning accuracy of the Hall sensor itself.

One of the tasks of the M1 magnet analysis was to evaluate the influence of its magnetic field on the beam of protons with an energy of 60.7 MeV (the main operating mode of the AIC-144 cyclotron) for beam's bending angle of 68°. There is no possibility of calculating the beam dynamics in the measured magnetic field map due to lack of a magnetic measurement

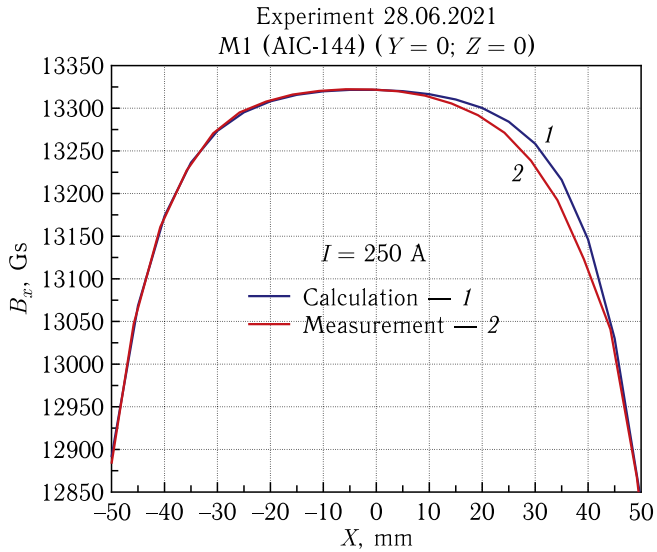

Fig. 14. Calculated and measured transverse magnetic fields of the M1 magnet in the experiment dated 28.06.2021

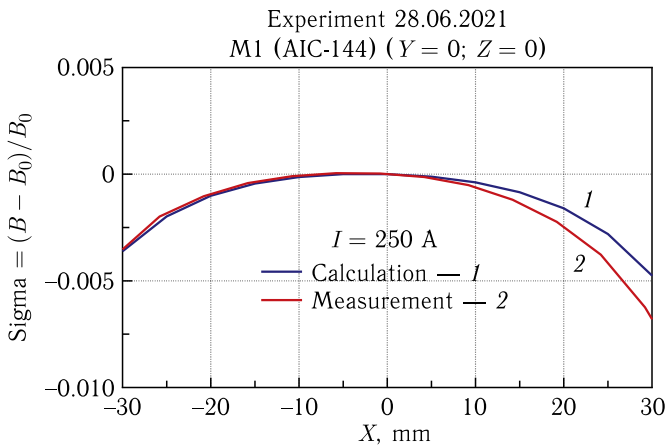

Fig. 15. Calculated and measured inhomogeneities of the M1 magnet's transverse magnetic field in the experiment dated 28.06.2021

system allowing magnetic measurements in a cylindrical coordinate system. Therefore, the beam dynamics can be calculated in the calculated magnetic field map only. In view of the fact that there is some difference between the calculated and measured values of the transverse magnetic field, the solution is to select the calculated configuration of the M1 magnet structure in which the distribution of the transverse magnetic field is close to the

measured values. The vertical profile of the M1 magnet pole was chosen so that the transverse magnetic field is similar to the measured one where simulated pole-to-pole gap of the M1 magnet is $h = (50.1 \pm 0.1)$ mm. It must be remembered that the measured pole-to-pole gap of the M1 magnet is $h = (50.03 \pm 0.05)$ mm. Thus, the magnetic field distortion due to unaccounted influence of vertical bar of the M1 magnet yoke is simulated by selecting vertical profile of the M1 magnet pole. After this, the transverse magnetic field in the working area, which is ±20 mm, coincides with good accuracy with the measured values and its inhomogeneity reaches $2.5 \cdot 10^{-3}$ in absolute value (Figs. 16 and 17).

The beam dynamics calculation was carried out using the SNOP program [3]. Trajectory analysis showed that for the deflection of protons with an energy of 60.7 MeV at an angle of 68° the central magnetic field's value (in the central point) should be 1.33 T (power supply current

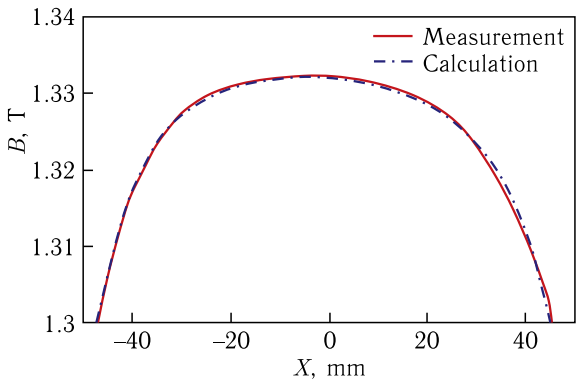

Fig. 16. Calculated (after selecting the pole profile) and measured transverse magnetic fields of the M1 magnet

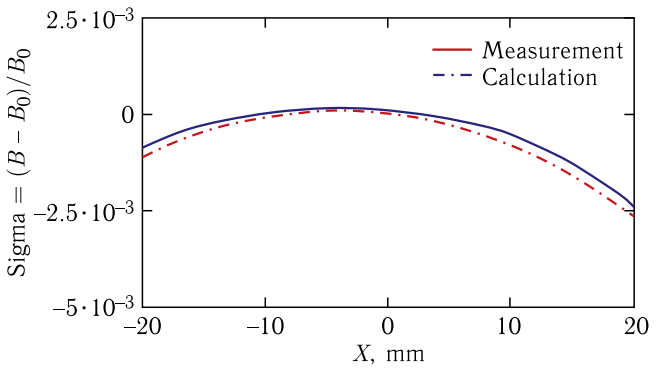

Fig. 17. Calculated (after selecting the pole profile) and measured inhomogeneities of the transverse magnetic field of the M1 magnet

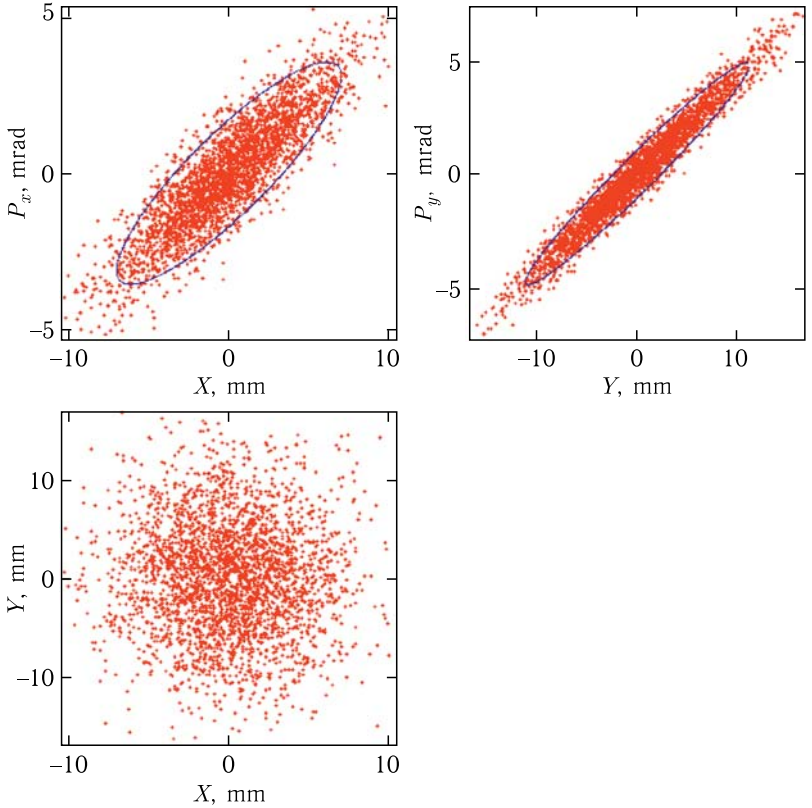

Fig. 18. Initial distribution of particles for beam dynamics calculation (600 mm before the beginning of the M1 magnet pole)

$\sim$ 250 A). For beam's bending angle of 68°, the central ion's trajectory will not pass along the arc with the radius of curvature of 840 mm (along the projection of the pole's center line on the median plane of the M1 magnet) throughout the entire M1 magnet, since the angular size of this dipole is 70°. To deflect protons at an angle of 70°, it is necessary to have a central magnetic field of 1.37 T (power supply current $\sim$ 270 A). The calculation of the particle beam motion was carried out with the value of transverse emittances $12\pi \cdot \text{mm} \cdot \text{mrad}$ and the beam spot sizes were taken according to the calculation results, which was performed using the Trace3D program [1] (Fig. 2). The initial distribution of particles for beam dynamics calculation is shown in Fig. 18.

The beam begins to move in the region where the M1 magnet's magnetic field is completely absent. Analysis of the beam dynamics in the configuration space shows (Fig. 19) that there are some distortions of the beam spot shape due to the effect of magnetic field nonlinearities, but there is no reason to

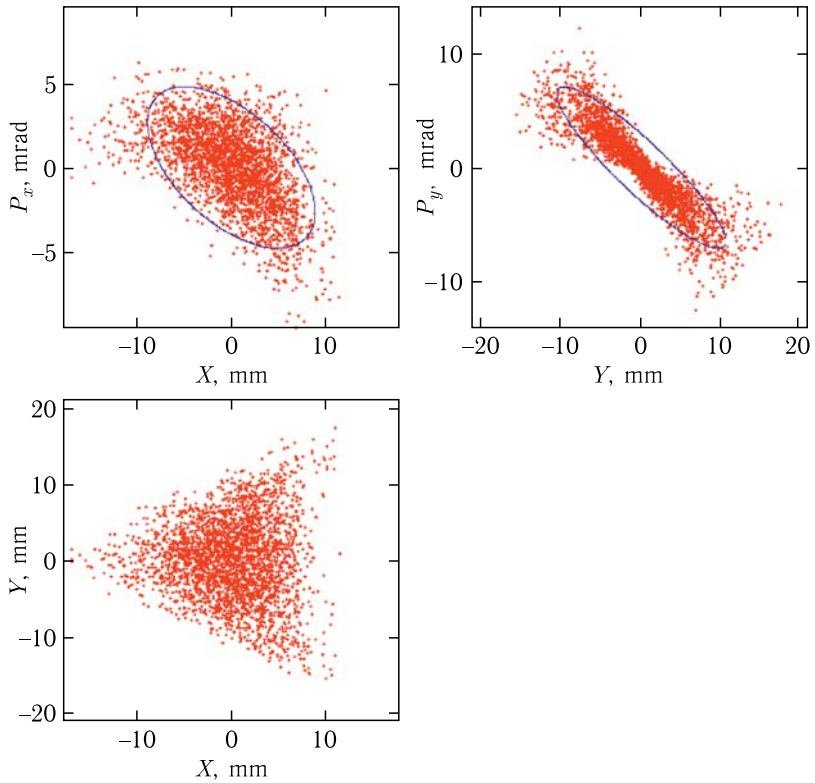

Fig. 19. Distribution of particles after passing the M1 magnet (600 mm after the ending of the M1 magnet pole)

believe that they will lead to noticeable negative consequences during further transportation of the beam. The beam spot sizes in the horizontal and vertical directions are similar, which meets the requirements.

CONCLUSIONS

The analysis of magnetic measurements of the M1 magnet showed that the value of inhomogeneity of the transverse magnetic field in the working area ± 20 mm in absolute value is $2.5 \cdot 10^{-3}$ with the requirements of $2.0 \cdot 10^{-3}$, which is acceptable.

The nonlinearities of the magnetic field lead to insignificant distortions of the beam spot shape, but the beam spot sizes in the horizontal and vertical directions are similar, which meets the requirements.

Thus, we can conclude that the work on production of the new M1 bending magnet was performed successfully.

Acknowledgments. The authors are grateful to N. A. Morozov for the technical task preparation and participation in manufacture of the new M1 bending magnet's yoke, to I. A. Ivanenko for the help in calibrating the Hall sensor, and to G. A. Karamysheva, chief of the Scientific and Experimental Department of New Accelerators, DLNP, JINR, for the support of the AIC-144 cyclotron project.

REFERENCES

1. https://laacg.lanl.gov/laacg/services/#trace3d
2. https://www.3ds.com/products-services/simulia/products/opera/
3. *Smirnov V. L., Vorozhtsov S. B.* SNOP — Beam Dynamics Analysis Code for Compact Cyclotrons // Proc. of the XXIII Russian Particle Accelerator Conference (RuPAC'2012), St. Petersburg, Russia, 2012. P. 325–327.

Received on December 9, 2021.

Редактор *Е. И. Кравченко*

Подписано в печать 04.02.2022.
Формат 60 × 90/16. Бумага офсетная. Печать цифровая.
Усл. печ. л. 1,0. Уч.-изд. л. 1,32. Тираж 180 экз. Заказ № 60349.

Издательский отдел Объединенного института ядерных исследований
141980, г. Дубна, Московская обл., ул. Жолио-Кюри, 6.
E-mail: publish@jinr.ru
www.jinr.ru/publish/